Microscopic origin of the different colors displayed by $MgAl_2O_4:Cr^{3+}$ and emerald

J. M. García-Lastra,[1] M. T. Barriuso,[2] J. A. Aramburu,[3] and M. Moreno[3]
[1]*Departamento de Física de Materiales, Facultad de Químicas, Universidad del País Vasco, 20018 San Sebastián, Spain*
[2]*Departamento de Física Moderna, Universidad de Cantabria, 39005 Santander, Spain*
[3]*Departamento de Ciencias de la Tierra y Física de la Materia Condensada, Universidad de Cantabria, 39005 Santander, Spain*
(Received 19 May 2008; revised manuscript received 4 July 2008; published 13 August 2008)

The difference in color between emerald ($Be_3Si_6Al_2O_{18}:Cr^{3+}$, green) and the Cr^{3+}-doped spinel $MgAl_2O_4$ (red) is striking, considering that in both systems color is due to CrO_6^{9-} complexes with a close local symmetry (D_3 and the D_{3d}, respectively) and that the measured Cr^{3+}-O^{2-} distance is practically the same (1.98 ± 0.01 and 1.97 ± 0.01 Å, respectively). By means of density-functional calculations it is shown that this surprising difference can reasonably be explained once the electric field, $\mathbf{E}_R$, which all lattice ions lying *outside* the CrO_6^{9-} complex exert on localized electrons, is taken into consideration. The origin of the different shape of $\mathbf{E}_R$ in the two host lattices is analyzed in detail. It is shown that $\mathbf{E}_R$ raises (decreases) the $2p$(O) levels for $Be_3Si_6Al_2O_{18}:Cr^{3+}$ ($MgAl_2O_4:Cr^{3+}$) along the trigonal axis thus favoring a decrease (increase) of $10Dq$. The present work demonstrates the key role played by $\mathbf{E}_R$ (not considered in the traditional ligand field theory) for understanding the differences exhibited by the same complex embedded in host lattices which do not have the same crystal structure. Some remarks on the color of Cr_2O_3 pure compound are also reported.

DOI: 10.1103/PhysRevB.78.085117 PACS number(s): 71.55.−i, 61.72.Bb, 71.15.Mb, 91.60.Mk

I. INTRODUCTION

A great deal of experimental work has been devoted to look into the properties of gemstones and minerals involving Cr^{3+}-doped oxides.[1–3] Despite these efforts the actual origin of the color exhibited by the different oxides lattices containing Cr^{3+} is still being debated.[3–10]

Historically, the optical properties of gemstones such as ruby (Cr^{3+}-doped corundum, Al_2O_3) and emerald (Cr^{3+}-doped beryl, $Be_3Si_6Al_2O_{18}$) have been interpreted in the framework of the traditional ligand field theory (LFT).[11,12] In this domain, it is assumed that the electronic properties of a transition-metal impurity, M, placed in an insulating lattice can be understood considering *only* the MX_N complex formed with the N nearest ions or ligands, X. The fact that crystal-field spectra of KMF_3 (M=Ni, Mn) pure compounds look very similar to those measured for $KMgF_3:M^{2+}$ (M=Ni, Mn) support such an assumption.[13–15] Along this line theoretical calculations on NiF_6^{4-}, MnF_6^{4-}, CrF_6^{3-}, or CrO_4^{4-} complexes *in vacuo* at the right experimental distance[16–20] is known to give values of optical transitions and electron-paramagnetic-resonance (EPR) parameters which are not far from experimental data[13–15,21,22] for $KMgF_3:M^{2+}$ (M=Ni, Mn), $K_2NaGaF_6:Cr^{3+}$, or $Mg_2SiO_4:Cr^{4+}$.

The idea of complex conveys a great simplification for understanding the electronic properties of transition-metal impurities in insulators. Thanks to it a problem in the realm of solid-state physics is reduced to study a relatively small *molecule* using *properly* the quantum mechanics. The validity of this idea was already discussed in the seminal paper by Sugano and Shulman[23] and is founded on two central points. The first key point is the localization of active electrons (coming from the transition-metal impurity) in the complex region, a fact well proved by EPR and electron-nuclear-double-resonance (ENDOR) spectra of transition-metal impurities in insulators and reproduced by theoretical calculations.[12] It is worth noting that the existence of localization in the total wave function is the fingerprint of an insulating material as it has been emphasized by Kohn.[24] Accordingly, if different atoms are involved in an insulating material the electronic localization favors the formation of ions. Therefore, even if electrons are well localized inside the complex region, the long-range Coulomb potential that every ion outside the complex exerts on active electrons cannot be forgotten.[25] Despite this fact, Sugano and Shulman[23] already showed that for a cubic perovskite lattice such as $KMgF_3$ the electrostatic potential, $V_R(\mathbf{r})$, due to all lattice ions lying outside the MF_6^{4-} complex (M=Ni, Mn, Co) is almost perfectly flat inside the complex and thus it can be ignored for understanding the associated optical transitions or EPR parameters. Accordingly, it has widely been *assumed* as another central point in the traditional LFT that the influence of $V_R(\mathbf{r})$ can be discarded for *every kind* of host lattice. If this idea is fully right the optical properties of an octahedral MX_N complex embedded in a series of different host lattices would depend only on the actual value of the *equilibrium* metal-ligand distance. This statement has been verified to be right looking at the different optical spectra of MnF_6^{4-}, NiF_6^{4-}, and CrF_6^{3-} complexes located in a series of distinct but *isomorphous* host lattices.[26–28]

By virtue of these facts the red and green color exhibited by ruby and emerald, respectively, have often been ascribed to a different value of the mean equilibrium Cr^{3+}-O^{2-} distance, R_I, in the CrO_6^{9-} complex.[1,2,29] Recent extended x-ray absorption fine structure (EXAFS) measurements carried out on ruby and emerald prove,[3,4,6,9] however, that the R_I value for both gemstones is the same within ± 0.01 Å.

The color of insulating oxides doped with Cr^{3+} essentially depends on the energy of the first spin allowed $^4A_{2g}(t_{2g}^3) \rightarrow {}^4T_{2g}(t_{2g}^2 e_g)$ transition[1,2,11,29] which is just equal to the cubic-field splitting parameter, $10Dq$, and thus independent on the Racah parameters. Within the traditional LFT it is assumed that

$$10Dq = (10Dq)_v, \tag{1}$$

where $(10Dq)_v$ stands for the complex *in vacuo*. Furthermore, it is assumed that $(10Dq)_v$ for a given octahedral complex only depends on the metal-ligand distance, R, through the law

$$(10Dq)_v = CR^{-n}, \tag{2}$$

where C is a constant. Optical absorption measurements under hydrostatic pressure carried out for $Al_2O_3:Cr^{3+}$ have shown[30] that experimental $10Dq$ values are reproduced by Eqs. (1) and (2) with $n=4.5$ and R means the mean Cr^{3+}-O^{2-} distance. Similar results have been obtained for other transition-metal complexes.[12,15] It is worth noting that for an octahedral complex pure crystal-field theory[11] gives $n=5$ although it leads to $10Dq$ values which are often one order of magnitude smaller than experimental ones.[12] The actual origin of the strong dependence of $(10Dq)_v$ upon R for octahedral complexes has been discussed[12,19,31,32] in a realistic molecular-orbital framework where ligands and the central cation are thus treated on the same footing. According to this analysis, since the work by Orgel,[33] the different color exhibited by ruby and emerald has been widely explained,[1,4,29] in the realm of the traditional LFT, *assuming* that R_I is about 5 pm higher for emerald than for ruby. This conclusion is, however, against recent experimental findings.[4,8,9]

A solution for understanding this somewhat puzzling situation has recently been put forward.[5,7,10] It has been argued that even if active electrons are well localized in the complex the electric field, $\mathbf{E}_R=-\nabla V_R(\mathbf{r})$, created by all ions of the insulating lattice lying *outside* the complex, on the electrons *in* the complex is not necessarily null at *every point of the complex region*. This means that all properties (and thus $10Dq$) associated with a complex do also depend on the shape of $\mathbf{E}_R$ in the complex region. In particular, emphasis has been placed on the importance of incorporating $\mathbf{E}_R(\mathbf{r})$ when comparing the properties of the same complex placed in two host lattices which are *not isomorphous*.

According to this new standpoint a difference between ruby and emerald comes out merely considering the local symmetry around the Cr^{3+} impurity. In fact, in $Al_2O_3:Cr^{3+}$ the local symmetry is C_3 and thus there is an electric field at the chromium site placed at $\mathbf{r}=0$. However, in the case of emerald the existence of two different symmetry axes in the local symmetry group (D_3) makes that $\mathbf{E}_R(0)$ is rigorously null.

A more subtle problem has recently been raised[8] in the comparison of emerald ($Be_3Si_6Al_2O_{18}:Cr^{3+}$) with the spinel $MgAl_2O_4$ doped with Cr^{3+}. In both cases the Cr^{3+} impurity enters the Al^{3+} site and the symmetry of the CrO_6^{9-} complex is relatively close. For $MgAl_2O_4:Cr^{3+}$ the local symmetry is D_{3d} and thus in this system, as well as in the emerald, the existence of an electric field at the chromium site is avoided by symmetry reasons. Recent EXAFS measurements[8,9] have led to a $R_I=1.97\pm0.01$ Å value for emerald while $R_I=1.98\pm0.01$ Å for $MgAl_2O_4:Cr^{3+}$. In spite of these facts the energy of the first spin allowed $^4A_{2g}(t_{2g}^3)\rightarrow{}^4T_{2g}(t_{2g}^2e_g)$ transition has been measured[1,34,35] to be equal to 18520 cm^{-1} for $MgAl_2O_4:Cr^{3+}$ while it is equal only to 16130 cm^{-1} for $Be_3Si_6Al_2O_{18}:Cr^{3+}$. This means that, although emerald and the spinel $MgAl_2O_4$ doped with Cr^{3+} exhibit a close local symmetry and have practically the same R_I value, the color displayed by $MgAl_2O_4:Cr^{3+}$ is red (identical to that of ruby for the human eye[29]) and not green.

The present work is aimed at clarifying this relevant issue by means of the same procedure previously employed[5,7] in the study of ruby, emerald and the two centers (with C_s and C_i symmetries) formed in alexandrite ($BeAl_2O_4:Cr^{3+}$). Accordingly, $10Dq$ is derived by means of density-functional calculations, considering the CrO_6^{9-} complex at the right equilibrium geometry and subject to the internal field, $\mathbf{E}_R(\mathbf{r})$, coming from the $MgAl_2O_4$ host lattice. For well clearing out the origin of differences between $MgAl_2O_4:Cr^{3+}$ and emerald, particular attention is paid to look into the shape of $\mathbf{E}_R(\mathbf{r})$ in the two $MgAl_2O_4$ and $Be_3Si_6Al_2O_{18}$ host lattices.

II. COMPUTATIONAL DETAILS

Due to the electronic localization *ab initio* calculations have been carried out on the CrO_6^{9-} complex in the framework of the density-functional theory (DFT) using the Amsterdam density-functional (ADF) code.[36] Particular attention has been paid to perform such calculations at the experimental equilibrium geometry[8,9] of every studied system.

As color displayed by Cr^{3+} doped oxides essentially depends on the energy of the $^4A_{2g}(t_{2g}^3)\rightarrow{}^4T_{2g}(t_{2g}^2e_g)$ transition,[1,2,11,29] efforts have been devoted to calculate $10Dq$ for $MgAl_2O_4:Cr^{3+}$ and emerald. For both systems, $10Dq$ has been computed for the complex *in vacuo* as well as including the effects of the electrostatic potential, $V_R(\mathbf{r})$, and thus there is not any fitting parameter in the present study.

The effects of $V_R(\mathbf{r})$ have been included by means of the same technique described in previous works.[5,7] In a first step, the electrostatic potential due to all ions of the $MgAl_2O_4$ or $Be_3Si_6Al_2O_{18}$ host lattices lying outside the CrO_6^{9-} cluster was calculated in 3071 points inside a sphere centered at the Cr^{3+} site and with a radius of 2.3 Å, slightly higher than the mean Cr^{3+}-O^{2-} distance at equilibrium. The electrostatic potential has been derived using a mixed Ewald-Evjen method where ion charges have been taken to be equal to the corresponding nominal charges. This assumption has been proved to be right[37] in the case of Al_2O_3. In a second step, the potential inside sphere has been reproduced using a small set of 196 effective charges lying outside the sphere. These charges are located at lattice positions although the charge values themselves are fitted in order to reproduce the right potential inside the sphere, with a maximum error in the potential of only 0.01%. Finally, this small set of fictitious charges was introduced into the ADF calculations.

The same functional and basis set are employed for calculating the emerald and the spinel. The generalized gradient approximation (GGA) exchange-correlation energy was computed using the Perdew-Wang functional,[38] PW91. It was verified that main results obtained in the present calculations are almost independent on the used functional. The Cr^{3+} ion has been described through basis sets of TZP (triple-ζ Slater-type orbitals STO plus one polarization function) quality given in the program database, keeping the core

TABLE I. Calculated $10Dq$ values for the CrO_6^{9-} complex *in vacuo* [at the experimental equilibrium geometry (Refs. 4, 8, and 9)] and under the internal electric field, $\mathbf{E}_R$, coming from $Be_3Si_6Al_2O_{18}$, $MgAl_2O_4$ and Al_2O_3 host lattices. The experimental $10Dq$ values of these systems (Refs. 1, 4, 34, and 35) are also enclosed. In the case of $MgAl_2O_4:Cr^{3+}$, $10Dq$ is given for the experimental distance (Ref. 8) ($R_I = 1.98 \pm 0.01$ Å) and also for $R = 1.995$ Å. In the case of ruby, R_I and R_H mean the average Cr^{3+}-O^{2-} and Al^{3+}-O^{2-} distance, respectively. R and R_H are given in Å while $10Dq$ in cm^{-1}.

System	R_H	R	$10Dq$ *in vacuo*	$10Dq$ Under $\mathbf{E}_R$	$10Dq$ Experimental
Emerald	1.906	1.975	16188	15739	16130
$MgAl_2O_4:Cr^{3+}$	1.930	1.980	16336	20627	18520
		1.995	15828	19996	
Ruby	1.913	1.965	16043	18179	18070

electrons ($1s$-$3p$) frozen. In the case of O^{2-} ions, a DZP (double-ζ Slater-type orbitals STO plus one polarization function) basis sets quality has been used, keeping the $1s$ shell frozen. This is the description for oxygen ions which has provided better agreement with experimental findings in recent works.[5,7,39]

In the DFT framework, properties directly depend on the electronic density, $\rho(\mathbf{r})$. For this reason DFT allows one to deal with fractional electronic charges. This possibility has been shown to be useful in the formulation of the concept of electronegativity[40] or for improving our understanding of the Jahn-Teller effect.[12,41,42] According to this view there is a simple way of getting a reasonable value of the energy, $E(a \rightarrow b)$, of the $a^1b^0 \rightarrow a^0b^1$ transition involving two different one-electron orbitals, a and b, with energies equal to ε_a and ε_b, respectively. It was first pointed out by Slater[43,44] that $E(a \rightarrow b)$ is essentially equal to $\varepsilon_b - \varepsilon_a$ where both ε_a and ε_b are calculated for a $a^{0.5}b^{0.5}$ state involving an equal but fractional occupation of the two electronic levels. Following this Slater's transition state concept,[43,44] a reasonable approximation to the value of the $10Dq$ parameter can be obtained through the average of configuration procedure described in Ref. 45. In the case of octahedral CrO_6^{9-} complexes the Kohn-Sham equations are solved for the average $t_{2g}^{9/5}e_g^{6/5}$ configuration where all mainly d levels are equally populated. As shown in Refs. 45 and 46, the difference between the $\varepsilon(e_g)$ and $\varepsilon(t_{2g})$ eigenvalues derived for such configuration with fractional occupation leads to a reasonable $10Dq$ value. This procedure can easily be extended if the symmetry of the complex is lower than O_h, such as happens in the present cases.

Let us shortly comment on the relation between the calculated $10Dq$ value and the peak of the $^4A_{2g}(t_{2g}^3) \rightarrow {}^4T_{2g}(t_{2g}^2e_g)$ absorption band. In $MgAl_2O_4:Cr^{3+}$ the existence of inversion symmetry in the D_{3d} symmetry group makes that such a transition is parity forbidden for electric-dipole selection rules assuming nuclei are frozen. However, this restriction is partially raised due to the vibronic interaction with an odd vibrational mode.[11] For this reason the associated band does not start, at $T=0$ K, at the zero-phonon line, E_{ZPL}, but at the so-called false origin[47,48] placed at $E_{ZPL}+h\nu_u$ where ν_u is the frequency of the odd local mode. For this reason the peak of the $^4A_{2g}(t_{2g}^3) \rightarrow {}^4T_{2g}(t_{2g}^2e_g)$ absorption band measured at a temperature T corresponds to $10Dq + h\nu_u \tanh(h\nu_u/2K_BT)$, where K_B is the Boltzmann constant. However, this shift is usually smaller than 200 cm^{-1} when bending odd modes are involved.[47,48]

III. RESULTS AND DISCUSSION

Seeking to look into the influence of the internal $\mathbf{E}_R(\mathbf{r})$ field on $10Dq$ and the color of $MgAl_2O_4:Cr^{3+}$ and emerald gemstones, calculations have been carried out in two steps. In the first one, $10Dq$ has been derived for the D_3 or D_{3d} CrO_6^{9-} complex *in vacuo* at the experimental equilibrium geometry thus considering the effects of small trigonal distortions. In a second step, the action of the internal electric field, $\mathbf{E}_R(\mathbf{r})$, upon active electrons in the complex is incorporated into the calculation. Main results are collected in Table I. In order to show the strong dependence of $10Dq$ upon R, calculated values for $MgAl_2O_4:Cr^{3+}$ at a distance $R = 1.995$ Å, very close to the experimental figure[8] $R_I = 1.98 \pm 0.01$ Å, have also been included in Table I. For the sake of completeness in that table, results for ruby are also reported, while values of the average Al^{3+}-O^{2-} distance in the perfect host lattices,[4,8,49] R_H, are enclosed for comparison purposes.

It is worth noting that for emerald and the spinel, the six Cr^{3+}-O^{2-} distances are equal although O^{2-}-Cr^{3+}-O^{2-} angles do not correspond to a perfect octahedron.[4,8,9,49] The departure from octahedral geometry is bigger for emerald than for $MgAl_2O_4:Cr^{3+}$. For instance, for two O^{2-} ions *in trans* position the O^{2-}-Cr^{3+}-O^{2-} angle is equal to 170.5° in the case of emerald while equal to 180° for spinel a fact which underlines its D_{3d} local symmetry. The existence of this trigonal distortion in the CrO_6^{9-} complex leads to small differences in the calculated $10Dq$ values for emerald and $MgAl_2O_4:Cr^{3+}$ when only the complex *in vacuo* is considered. Let us call $\Delta_{SE} = 10Dq(MgAl_2O_4:Cr^{3+}) - 10Dq(\text{emerald})$. As shown in Table I the calculated value for the complex *in vacuo* is $\Delta_{SE} \sim 300$ cm^{-1} and thus it is eight times smaller than the experimental value $\Delta_{SE} = 2390$ cm^{-1}.

Looking at the results gathered in Table I it is also hard to understand the distinct $10Dq$ values exhibited by $MgAl_2O_4:Cr^{3+}$ and emerald through the complex *in vacuo* even if the uncertainty in the experimental R_I value (± 0.01 Å) is considered. In fact, as $R_H = 1.93$ Å for the spi-

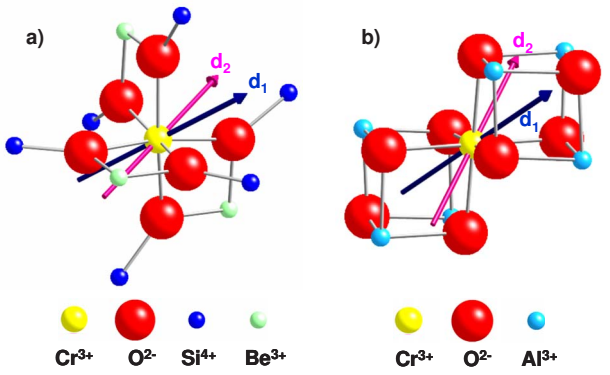

FIG. 1. (Color online) CrO_6^{9-} complexes and their surrounding shells of neighbors in (a) the emerald and (b) in the spinel. The meaning of the directions d_1 and d_2 is explained in the text and in Fig. 3.

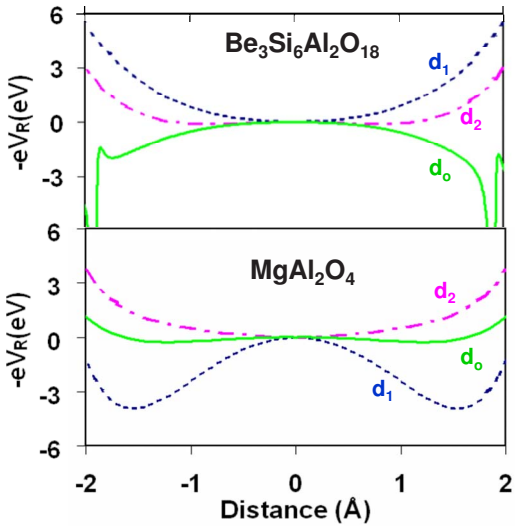

FIG. 2. (Color online) (a) Electrostatic potential $V_R(\mathbf{r})$ of the rest of the lattice ions on a CrO_6^{9-} complex for the case of emerald (above) and spinel (below), depicted along d_0, d_1, and d_2 directions. The meaning of the three directions is explained in the text and in Fig. 3.

nel while R_H=1.906 Å for beryl, it can reasonably be expected that $R_I(MgAl_2O_4:Cr^{3+}) \geq R_I$(emerald) according to the general behavior observed when a given complex is inserted in different host lattices.[12,26] In fact, for 3*d* complexes placed in a series of cubic insulating lattices it has been found that R_I values are ordered in the same way as R_H. Bearing in mind these facts, Eq. (1) and the results of Table I it can be concluded that if we only consider the complex *in vacuo* Δ_{SE} is expected to be smaller than 300 cm^{-1}.

As shown in Table I, a significant *increase* on the calculated $10Dq$ value of $MgAl_2O_4:Cr^{3+}$ is obtained once the corresponding internal electric field, $\mathbf{E}_R(\mathbf{r})$, is incorporated into the calculation. In agreement with what was previously reported,[5,7] $\mathbf{E}_R(\mathbf{r})$ is found to *reduce* but only by ~450 cm^{-1} the $10Dq$ value derived for emerald using a complex *in vacuo*. Therefore, the variation on $10Dq$ induced by $\mathbf{E}_R(\mathbf{r})$ in this gemstone has a different sign to that in $MgAl_2O_4:Cr^{3+}$. These results just mean that when the complex is inserted in a lattice there is a *supplementary* contribution to $10Dq$ coming from $V_R(\mathbf{r})$, termed as Δ_R, and thus Eq. (1) has to be modified as follows[10]

$$10Dq = (10Dq)_v + \Delta_R. \tag{3}$$

It has recently been pointed out that Δ_R plays a relevant role even if host lattices are cubic.[50] The results gathered in Table I then support that the internal $\mathbf{E}_R(\mathbf{r})$ field plays a key role for understanding why $MgAl_2O_4:Cr^{3+}$ is red despite the local symmetry around Cr^{3+} is D_{3d}, not far from that for the emerald. Despite this fact the results embodied in Table I and those previously obtained[5,7,50] stress that the main contribution to $10Dq$ comes from $(10Dq)_v$.

An insight into the origin of such a difference can be gained looking at Fig. 1, where the arrangement of neighbor ions to the CrO_6^{9-} complex can be seen for both $MgAl_2O_4$ and $Be_3Si_6Al_2O_{18}$ host lattices. In both cases the direction called d_1 in Fig. 1 corresponds to the C_3 axis in D_3 or D_{3d} symmetry. Despite both lattices have a close local symmetry around Cr^{3+} the nature and arrangement of first and second shell of ions looks certainly different. In the case of $MgAl_2O_4$ the second shell around the central Al_c^{3+} ion (which is replaced by the Cr^{3+} impurity) is composed[49] by six Al^{3+} ions placed at 2.86 Å, while the third shell is formed by two O^{2-} ions lying at 3.33 Å. All these ions are shown in Fig. 1. Next there are six Mg^{2+} located at 3.35 Å and six O^{2-} ions at 3.56 Å while further shells are all lying at a distance higher than 4 Å. Differences between the local geometry in $MgAl_2O_4$ and $Be_3Si_6Al_2O_{18}$ are already visible looking at the second shell. In fact, in $Be_3Si_6Al_2O_{18}$ there are only three Be^{3+} ions lying at 2.66 Å from the central Al_c^{3+} ion involved in this shell.[4,9] Further differences between two lattices appear considering the angle, ϕ_3, formed by an Al_c^{3+}-M_{2s}^{3+} direction with the principal C_3 axis. Here M_{2s}^{3+} just means a cation of the second shell. While ϕ_3=90° for beryl lattice, ϕ_3 is equal only to 35.26° for the spinel. As shown in Fig. 1 six Si^{4+} ions, at 3.28 Å from Al_c^{3+}, are involved in the third shell of $Be_3Si_6Al_2O_{18}$. The fourth shell is composed by six O^{2-} ions at 3.73 Å from Al_c^{3+}.

Bearing in mind the structural differences between the spinel and the beryl lattices let us now have a look at the form of the calculated $\mathbf{E}_R$ field in the two lattices. For seeing in what places of the complex region there is an electric field $\mathbf{E}_R(\mathbf{r}) \neq 0$ it is useful to portray the potential $V_R(\mathbf{r})$ generating $\mathbf{E}_R$. The form of the $(-e)[V_R(\mathbf{r}) - V_R(0)]$ function along several directions is drawn for both lattices in Fig. 2. For clarifying what are the chosen directions and especially the nature of involved electronic orbitals it is convenient to work also with the trigonal basis (x_t, y_t, z_t) defined in Fig. 3. Quantities referred to this basis will be denoted by the subscript *t*.

In Fig. 2 the form of $(-e)V_R(\mathbf{r})$ is depicted for directions called d_0, d_1, and d_2. Here d_1 and d_2 correspond to $\langle 0,0,1\rangle_t$ and $\langle -1,1,\sqrt{2}\rangle = \langle \sqrt{3}, \sqrt{2}, 1\rangle_t$ directions, respectively, while d_0 refers to a metal-ligand direction corresponding to $\langle 1,0,0\rangle$ type directions in the $\{x,y,z\}$ basis set (Fig. 3). These directions will be useful in the later discussion.

Although, according to both D_3 and D_{3d} symmetries, $\mathbf{E}_R(0)=0$ the shape of the $(-e)V_R(\mathbf{r})$ function looks quite

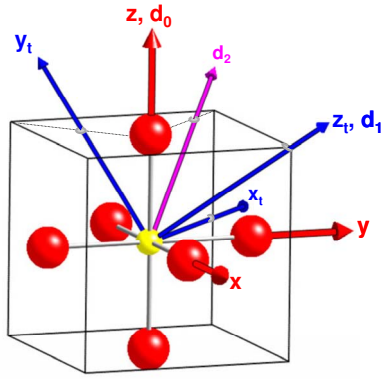

FIG. 3. (Color online) Main axis of an octahedral basis $\{x,y,z\}$ and in a trigonal basis $\{x_t,y_t,z_t\}$ related by $x_t=(1/\sqrt{2})(-x+y)$,$y_t=(1/\sqrt{6})(-x-y+2z)$, $z_t=(1/\sqrt{3})(x+y+z)$. d_1 and d_3 directions coincide with z_t and x_t, respectively, while d_2 is written as $d_2=-(1/2)x+(1/2)y+(1/\sqrt{2})z$ in the octahedral basis or equivalently $d_2=(1/\sqrt{2})x_t+(1/\sqrt{3})y_t+(1/\sqrt{6})z_t$ in the trigonal basis.

different at the ligand region for the two considered host lattices (Fig. 2). For instance, along the d_1 direction of $Be_3Si_6Al_2O_{18}$ the $(-e)V_R(\mathbf{r})$ function shows an *increase* of about 1 eV from the origin to the $\mathbf{r}=(0,0,1)_t$ Å point, while for $MgAl_2O_4$ there is a *lessening* of 3 eV. As regards a metal-ligand direction, d_0, $(-e)V_R(\mathbf{r})$ decreases but slightly for beryl while it is practically flat for the spinel. The distinct shape of $(-e)V_R(\mathbf{r})$ along d_1 is qualitatively consistent with the quite different value of the ϕ_3 angle for $MgAl_2O_4$ and $Be_3Si_6Al_2O_{18}$. Considering the spinel lattice, if the electron moves from the central position along a $\langle 0,0,1\rangle_t$ direction it is attracted toward the closer plane of three Al^{3+} ions (Fig. 1). By contrast, in beryl the three Be^{3+} ions of the second shell are lying in a plane perpendicular to the d_1 direction (C_3 axis) and thus $(-e)[V_R(\mathbf{r})-V_R(0)]$ should behave in an opposite way.

The different $10Dq$ values exhibited by $MgAl_2O_4:Cr^{3+}$ and emerald can qualitatively be understood just considering the effects of $(-e)V_R(\mathbf{r})$ upon $e_g(\sim x^2-y^2,\ 3z^2-r^2)$ and $t_{2g}(\sim xy,\ xz,\ yz)$ orbitals in first-order perturbation. In fact, at least ~80% of the $10Dq$ value is already obtained through a calculation of the complex *in vacuo* (Table I).

Let us first consider the antibonding $e_g(\sim x^2-y^2,\ 3z^2-r^2)$ orbitals in cubic symmetry. It should be recalled here that although such orbitals transform like x^2-y^2 and $3z^2-r^2$ wave functions of central cation the actual molecular-orbital wave functions involves an admixture with $2p$ and $2s$ wave functions of oxygen ligands. As the degeneracy in e_g is not removed by a trigonal distortion, we can consider that in the present cases such orbitals describe in a first approximation the e orbitals in D_3 symmetry. Bearing in mind that $e_g(\sim x^2-y^2,\ 3z^2-r^2)$ orbitals are mainly directed toward ligands (d_o directions) and looking at Fig. 2, it can be expected that $\mathbf{E}_R$ has practically no effect for $MgAl_2O_4:Cr^{3+}$ while it would induce a decrease of the energy of such orbitals in the case of the emerald thus favoring a lessening of $10Dq$. It should be remarked that, in order to interpret Fig. 2, such effect depends on the probability of finding an e_g electron on ligands and thus on the covalency of the chemical bonding between

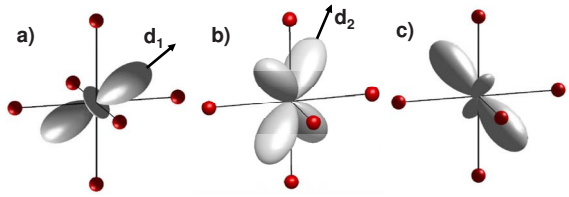

FIG. 4. (Color online) Orbitals belonging to the t_{2g} triplet in a D_3 symmetry. (a) Singlet orbital a. It is written as $(xy+xz+yz)$ in the octahedral basis and $3z_t^2-r_t^2$ in the trigonal basis. (b) First of the orbitals of the doublet e. It is written as $(xz-yz)$ in the octahedral basis and $(\sqrt{2}x_ty_t+x_tz_t)$ in the trigonal basis. (c) Second of the orbitals of the doublet e. It is written as $(xz+yz-2xy)$ in the octahedral basis and $(x_t^2-y_t^2+\sqrt{2}\ y_tz_t)$ in the trigonal basis. The meaning of the directions d_1 and d_2 is explained in the text and in Fig. 3.

chromium and oxygen ligands. Present calculations give a total charge on ligands equal to 25% (14%) for an electron in an e_g (t_{2g}) orbital.

More interesting effects appear precisely in the case of t_{2g} $(\sim xy,\ xz,\ yz)$ orbitals in cubic symmetry. First of all, the trigonal distortion splits t_{2g} into a singlet a and a doublet e in D_3 symmetry. Under D_{3d} symmetry these orbitals should properly be called a_g and e_g but this matter will not be taken into consideration in the following discussion. The wave function of the a singlet transforms like $(xy+xz+yz)$, that is, $3z_t^2-r_t^2$ in the trigonal basis (Fig. 3). This means that the a orbital is directed along the C_3 axis although some density is also located in the perpendicular plane (Fig. 4). As regards the $e(t_{2g})$ doublet the two orbitals forming the basis can be chosen as $(xz-yz)\sim(\sqrt{2}x_ty_t+x_tz_t)$ and $(xz+yz-2xy)\sim(x_t^2-y_t^2+\sqrt{2}y_tz_t)$. Considering the $(xz-yz)\sim(\sqrt{2}x_ty_t+x_tz_t)$ orbital of the $e(t_{2g})$ doublet it involves an admixture of the x_ty_t orbital, lying in the perpendicular plane to the C_3 axis, with the x_tz_t lying outside that plane. The $(xz-yz)\sim(\sqrt{2}x_ty_t+x_tz_t)$ orbital possesses four lobes, two placed along $\langle -1,1,\sqrt{2}\rangle=\langle\sqrt{3},\sqrt{2},1\rangle_t$ and two along $\langle 1,-1,\sqrt{2}\rangle=\langle-\sqrt{3},\ \sqrt{2},\ 1\rangle_t$ direction. Bearing in mind these considerations it is possible to understand the different influence of $(-e)V_R(\mathbf{r})$ on $t_{2g}(\sim xy,\ xz,\ yz)$ orbitals in the two host lattices. Let us first consider the $a(t_{2g})$ orbital. Looking at Figs. 2 and 4 it is clear that in the case of emerald the electronic density lying around $\langle 0,0,1\rangle_t$ increases its energy due to the action of $V_R(\mathbf{r})$. By contrast, for the spinel the electronic density located in the neighborhood of $\mathbf{r}=\langle 0,0,1.5\rangle_t$Å is subject to $(-e)[V_R(\mathbf{r})-V_R(0)]\approx-3$ eV, which tends to decrease the energy of the $a(t_{2g})$ orbital. In Fig. 2 is also portrayed the form of $V_R(\mathbf{r})$ along a d_2 direction corresponding to one of the lobes of the $(xz-yz)\sim(\sqrt{2}x_ty_t+x_tz_t)$ orbital. It can be noticed that for both $MgAl_2O_4:Cr^{3+}$ and emerald, $(-e)V_R(\mathbf{r})$ is practically constant for $|\mathbf{r}|<1.5$ Å, although it increases slightly for higher distances. In view of these considerations, it can be expected that the energy of the t_{2g} barycenter of the emerald is increased with respect to that of the spinel due to the action of the internal electric field. This fact helps again to lessen the value of $10Dq$ in the former case and to enhance it in the latter one. The present argument is thus in qualitative agreement with the calculated values shown in Table I.

IV. FINAL REMARKS

The present study shows that the different color of $MgAl_2O_4:Cr^{3+}$ and emerald can be well explained just considering the CrO_6^{9-} complex subject to the corresponding internal field $\mathbf{E}_R$. This result is thus consistent with previous studies carried out on Cr^{3+}-doped oxides.[7,10] Along this line it has recently been pointed out that the shift undergone by crystal-field and charge transitions of Cr^{3+} and Fe^{3+} impurities on passing from beryl to corundum can also be ascribed to the different shape of $\mathbf{E}_R$ in the two host lattices.[51]

In principle periodic *ab initio* calculations performed on a big supercell would be able to reproduce both the right R_I and $10Dq$ values for both $MgAl_2O_4:Cr^{3+}$ and $Be_3Si_6Al_2O_{18}:Cr^{3+}$. Apart from its high computational cost it is not simple to understand *only* by means of those calculations what is the *main physical cause* behind the different color of $MgAl_2O_4:Cr^{3+}$ and $Be_3Si_6Al_2O_{18}:Cr^{3+}$. Moreover it is not sure that calculations of this kind would be able to reproduce the 13% reduction in $10Dq$ on passing from $MgAl_2O_4:Cr^{3+}$ to emerald due to the errors in the computed R_I values. In fact, the difference between computed and experimental R_I values is usually at least of $\pm 1\%$. Nevertheless this small uncertainty on R_I can lead to errors in $(10Dq)_v$ which are already at least of $\pm 5\%$ for each system considering the strong dependence of $(10Dq)_v$ upon R. This problem is, however, avoided in the present study where R_I values are taken from experiments.

Although the local symmetry around the impurity in $MgAl_2O_4:Cr^{3+}$ and emerald is close (D_{3d} and D_3, respectively), however, the arrangement of near ions and consequently the behavior of $V_R(\mathbf{r})$ is quite different in both lattices as stressed by Figs. 1 and 2. It is worth remarking here that the importance of $V_R(\mathbf{r})$ in the present problem is enhanced due to the *directionality* of orbitals. By virtue of this fact, the electronic density in e_g and t_{2g} orbitals is not isotropically distributed in the complex region.

The present calculations gathered in Table I lead to a $10Dq$ value for $MgAl_2O_4:Cr^{3+}$ which is higher than that for ruby. Although this is in qualitative agreement with experiments,[1–3,34,35] the observed difference in $10Dq$ between both systems, Δ_{SR}, is only of 450 cm^{-1}, and thus this difference is overestimated by the present calculations leading to $\Delta_{SR}=2600$ cm^{-1} using $R_I=1.98$ Å for $MgAl_2O_4:Cr^{3+}$ (Table I). Apart from the fact that discrepancies between experimental and calculated $10Dq$ values of about 1000 cm^{-1} are very common, there are two factors that could contribute to reduce this overestimation. On one hand, if there is an experimental uncertainty of ± 0.01 Å for each system this could lead to a decrease of 1000 cm^{-1} in Δ_{SR}. On the other hand, the calculated splitting between $e_g(t_{2g})$ and $a_g(t_{2g})$ orbitals for $MgAl_2O_4:Cr^{3+}$ is ~ 2600 cm^{-1} which is not observed experimentally. We have verified that this splitting is greatly due to a 25% contamination of $4s$ orbitals in the singlet $a_g(t_{2g})$ which lies below $e_g(t_{2g})$. If this anomaly is eliminated this would decrease $10Dq$ by ~ 600 cm^{-1}.

The present results underline that the difference Δ_{SE} can reasonably be understood considering the effects of the corresponding $V_R(\mathbf{r})$ potential in first-order perturbation. In essence, this statement just means that the changes in electronic density associated with $V_R(\mathbf{r})$ are relatively small. This idea is confirmed looking at the position of the sharp $^2E_g(t_{2g}^3) \rightarrow {}^4A_{2g}(t_{2g}^3)$ emission transition, which basically depends on Racah parameters and thus on the electronic density.[1,2,11] This transition is observed at 14690 cm^{-1} for emerald[1] while in the case of $MgAl_2O_4:Cr^{3+}$ it is shifted[21] by only 0.2% to lower energies.

Let us now say a few words on the green color displayed by the Cr_2O_3 pure compound[52,53] which has the same structure as Al_2O_3. Compared to $Al_2O_3:Cr^{3+}$ ($10Dq=18070$ cm^{-1}), the value $10Dq=16700$ cm^{-1} measured[52] for Cr_2O_3 involves a shift $\Delta(10Dq)=-1370$ cm^{-1}. Recent EXAFS measurements[6] give a mean distance $R_I=1.965\pm 0.01$ Å for ruby while $R_I=1.98\pm 0.01$ Å for Cr_2O_3. According to Eq. (2), one would expect that on going from $Al_2O_3:Cr^{3+}$ to Cr_2O_3, the $(10Dq)_v$ quantity would decrease by ~ 600 cm^{-1}. Nevertheless, this figure is about half the experimental value $\Delta(10Dq)=-1370$ cm^{-1}. The $\Delta(10Dq)$ quantity is likely to be influenced[53] by the superexchange interaction among two close chromium ions in Cr_2O_3. Apart from this fact, it is worth noting that while in Al_2O_3 the charge on aluminum is found[37] to be practically equal to +3 the charge on chromium in Cr_2O_3 is expected to be smaller as a result of the covalent bonding which is always present in every transition-metal complex. As shown in Sec. II, 14% of the electronic charge associated with an electron in an antibonding t_{2g} orbital is found to be placed on ligands. The expected reduction on the absolute value of metal and oxygen charges on passing from Al_2O_3 to Cr_2O_3 would tend to decrease the value of $|V_R(\mathbf{r})-V_R(0)|$ and thus the Δ_R contribution. Along this line, it has been shown[5] that if in the Al_2O_3 lattice the cation charge goes from +3 to +2.7 it induces a Δ_R lessening of 550 cm^{-1}. Work on this subject deserves a further investigation which is currently under way.

ACKNOWLEDGMENTS

The authors would like to thank to A. Juhin who suggested exploring the present problem. The support by the Spanish Ministerio de Ciencia y Tecnología under Project FIS2006-02261 is also acknowledged.

[1] R. G. Burns, *Mineralogical Applications of Crystal Field Theory* (Cambridge University Press, Cambridge, England, 1993).
[2] R. C. Powell, *Physics of Solid State Laser Materials* (Springer, New York, 1998).
[3] E. Gaudry, PhD thesis, Université Paris VI, 2004.
[4] E. Gaudry, A. Kiratisin, P. Sainctavit, C. Brouder, F. Mauri, A. Ramos, A. Rogalev, and J. Goulon, Phys. Rev. B **67**, 094108 (2003).
[5] J. M. Garcia-Lastra, M. T. Barriuso, J. A. Aramburu, and M. Moreno, Phys. Rev. B **72**, 113104 (2005).
[6] E. Gaudry, P. Sainctavit, F. Juillot, F. Bondioli, P. Ohresser, and I. Letard, Phys. Chem. Miner. **32**, 710 (2006).
[7] J. M. García-Lastra, J. A. Aramburu, M. T. Barriuso, and M. Moreno, Phys. Rev. B **74**, 115118 (2006).
[8] A. Juhin, G. Calas, D. Cabaret, L. Galoisy, and J. L. Hazemann, Phys. Rev. B **76**, 054105 (2007).
[9] E. Gaudry, D. Cabaret, C. Brouder, I. Letard, A. Rogalev, F. Wilhlem, N. Jaouen, and P. Sainctavit, Phys. Rev. B **76**, 094110 (2007).
[10] M. Moreno, M. Garcia-Lastra, M. T. Barriuso, and J. A. Aramburu, Theor. Chem. Acc. **118**, 665 (2007).
[11] S. Sugano, Y. Tanabe, and H. Kamimura, *Multiplets of Transition-Metal Ions in Crystals* (Academic, New York, 1970), Vol. 33, p. 331.
[12] M. Moreno, M. T. Barriuso, J. A. Aramburu, P. Garcia-Fernandez, and J. M. Garcia-Lastra, J. Phys.: Condens. Matter **18**, R315 (2006).
[13] K. Knox, S. Sugano, and R. G. Shulman, Phys. Rev. **130**, 512 (1963).
[14] V. Goldberg, R. Moncorge, D. Pacheco, and B. DiBartolo, *Luminescence of Inorganic Solids* (Plenum, New York, 1988).
[15] M. C. Marco de Lucas, F. Rodriguez, and M. Moreno, Phys. Rev. B **50**, 2760 (1994).
[16] A. J. Wachters and W. C. Nieuwpoort, Phys. Rev. B **5**, 4291 (1972).
[17] M. Florez, L. Seijo, and L. Pueyo, Phys. Rev. B **34**, 1200 (1986).
[18] M. T. Barriuso, J. A. Aramburu, M. Moreno, M. Florez, G. F. Rodrigo, and L. Pueyo, Phys. Rev. B **38**, 4239 (1988).
[19] K. Wissing, M. T. Barriuso, J. A. Aramburu, and M. Moreno, J. Chem. Phys. **111**, 10217 (1999).
[20] L. Pueyo and J. W. Richardson, J. Chem. Phys. **67**, 3583 (1977).
[21] D. L. Wood, J. F. Dillon, K. Knox, and J. Ferguson, J. Chem. Phys. **39**, 890 (1963).
[22] M. F. Hazenkamp, H. U. Gudel, M. Atanasov, U. Kesper, and D. Reinen, Phys. Rev. B **53**, 2367 (1996).
[23] S. Sugano and R. G. Shulman, Phys. Rev. **130**, 517 (1963).
[24] W. Kohn, in *Many Body Physics*, edited by C. Witt and R. Balian (Gordon and Breach, New York, 1968).
[25] W. Kohn, Phys. Rev. Lett. **76**, 3168 (1996).
[26] M. T. Barriuso, J. A. Aramburu, and M. Moreno, J. Phys.: Condens. Matter **11**, L525 (1999).
[27] B. Villacampa, R. Cases, V. M. Orera, and R. Alcala, J. Phys. Chem. Solids **55**, 263 (1994).
[28] C. Marco de Lucas, F. Rodríguez, J. M. Dance, M. Moreno, and A. Tressaud, J. Lumin. **48-49**, 553 (1991).
[29] K. Nassau, *The Physics and Chemistry of Colour* (Wiley, New York, 1983).
[30] S. J. Duclos, Y. K. Vohra, and A. L. Ruoff, Phys. Rev. B **41**, 5372 (1990).
[31] M. Moreno, J. A. Aramburu, and M. T. Barriuso, Phys. Rev. B **56**, 14423 (1997).
[32] P. Garcia-Fernandez, J. M. Garcia-Lastra, J. A. Aramburu, M. T. Barriuso, and M. Moreno, Chem. Phys. Lett. **426**, 91 (2006).
[33] L. E. Orgel, Nature (London) **179**, 1348 (1957).
[34] D. L. Wood, G. F. Imbusch, R. M. Macfarland, P. Kisliuk, and D. M. Larkin, J. Chem. Phys. **48**, 5255 (1968).
[35] D. T. Sviridov, B. K. Sevastya, V. P. Orekhova, R. K. Sviridov, and T. F. Veremeic, Opt. Spektrosk. **35**, 102 (1973).
[36] G. te Velde, F. M. Bickelhaupt, E. J. Baerends, C. F. Guerra, S. J. A. Van Gisbergen, J. G. Snijders, and T. Ziegler, J. Comput. Chem. **22**, 931 (2001).
[37] C. Sousa, C. de Graaf, and F. Illas, Phys. Rev. B **62**, 10013 (2000).
[38] J. P. Perdew, J. A. Chevary, S. H. Vosko, K. A. Jackson, M. R. Pederson, D. J. Singh, and C. Fiolhais, Phys. Rev. B **46**, 6671 (1992).
[39] J. A. Aramburu, J. M. Garcia-Lastra, M. T. Barriuso, and M. Moreno, Int. J. Quantum Chem. **91**, 197 (2003).
[40] R. G. Parr and W. Yang, *Density Functional Theory of Atoms and Molecules* (Oxford University Press, New York, 1989).
[41] M. T. Barriuso, P. Garcia-Fernandez, J. A. Aramburu, and M. Moreno, Solid State Commun. **120**, 1 (2001).
[42] J. M. Garcia-Lastra, M. T. Barriuso, J. A. Aramburu, and M. Moreno, Chem. Phys. **317**, 103 (2005).
[43] J. C. Slater, Adv. Quantum Chem. **6**, 1 (1972).
[44] J. C. Slater, *The Self-Consistent Field for Molecules and Solids* (McGraw-Hill, New York, 1974).
[45] M. Atanasov, C. Daul, and C. Rauzy, Struct. Bonding (Berlin) **106**, 97 (2004).
[46] H. Adachi, S. Shiokawa, M. Tsukada, C. Satoko, and S. Sugano, J. Phys. Soc. Jpn. **47**, 1528 (1979).
[47] R. Knochenmuss, C. Reber, M. V. Rajasekharan, and H. U. Gudel, J. Chem. Phys. **85**, 4280 (1986).
[48] J. M. García-Lastra, M. Moreno, and M. T. Barriuso, J. Chem. Phys. **128**, 144708 (2008).
[49] T. Yamanaka and Y. Takeuchi, Z. Kristallogr. **165**, 65 (1983).
[50] J. M. Garcia-Lastra, J. Y. Buzare, M. T. Barriuso, J. A. Aramburu, and M. Moreno, Phys. Rev. B **75**, 155101 (2007).
[51] G. Spinolo, I. Fontana, and A. Galli, Phys. Status Solidi B **244**, 4660 (2007).
[52] D. Reinen, Struct. Bonding (Berlin) **6**, 30 (1969).
[53] M. G. Brik, N. M. Avram, and C. N. Avram, Solid State Commun. **132**, 831 (2004).